Carbohydrate Polymers 90 (2012) 1147–1158

Contents lists available at SciVerse ScienceDirect

Carbohydrate Polymers

journal homepage: www.elsevier.com/locate/carbpol

Physical properties of emulsion-based hydroxypropyl methylcellulose films: Effect of their microstructure

R.N. Zúñiga[a,*], O. Skurtys[b], F. Osorio[c], J.M. Aguilera[a], F. Pedreschi[a]

[a] Department of Chemical and Bioprocesses Engineering, Pontificia Universidad Católica de Chile, Avenida Vicuña Mackenna 4860, Macul, Santiago, Chile
[b] Department of Mechanical Engineering, Universidad Técnica Federico Santa María, Avenida Vicuña Mackenna 3939, San Joaquín, Santiago, Chile
[c] Department of Food Science and Technology, Universidad de Santiago de Chile, Avenida Ecuador 3769, Estación Central, Santiago, Chile

ARTICLE INFO

Article history:
Received 25 March 2012
Received in revised form 20 June 2012
Accepted 24 June 2012
Available online 2 July 2012

Keywords:
Emulsion
Edible films
Microstructure
Destabilization
Physical properties

ABSTRACT

The initial characteristics of emulsions and the rearrangement of the oil droplets in the film matrix during film drying, which defines its microstructure, has an important role in the physical properties of the emulsion-based films. The objective of this work was to study the effect of the microstructure (two droplet size distributions) and stability (with or without surfactant) of HPMC oil-in-water emulsions over physical properties of HPMC emulsion-based edible films. HPMC was used to prepare sunflower oil-in-water emulsions containing 0.3 or 1.0% (w/w) of oil with or without SDS, as surfactant, using an ultrasonic homogenizer. Microstructure, rheological properties and stability of emulsions (creaming) were measured. In addition, microstructure, coalescence of oil droplets, surface free energy, optical and mechanical properties and water vapor transfer of HPMC films were evaluated. Image analysis did not show differences among droplet size distributions of emulsions prepared at different oil contents; however, by using SDS the droplet size distributions were shifted to lower values. Volume mean diameters were 3.79 and 3.77 μm for emulsions containing 0.3 and 1.0% without surfactant, respectively, and 2.72 and 2.71 μm for emulsions with SDS. Emulsions formulated with 1.0% of oil presented higher stability, with almost no change during 5 and 3 days of storage, for emulsions with and without SDS, respectively. Internal and surface microstructure of emulsion-based films was influenced by the degree of coalescence and creaming of the oil droplets. No effect of microstructure over the surface free energy of films was found. The incorporation of oil impaired the optical properties of films due to light scattering of light. Addition of oil and SDS decreased the stress at break of the emulsion-based films. The replace of HPMC by oil and SDS produce a lower "amount" of network structure in the films, leading to a weakening of their structure. The oil content and SDS addition had an effect over the microstructure and physical properties of HPMC-based emulsions which lead to different microstructures during film formation. The way that oil droplets were structured into the film had an enormous influence over the physical properties of HPMC films.

1. Introduction

An edible film is defined as a thin layer of material, which can be eaten as part of the whole product, providing a barrier to mass transfer (moisture, gas, flavors, *etc.*) between the food and the surrounding environment or in the food itself, for instance between compartments of different water activities in the same food (Borlieu, Guillard, Vallès-Pamiès, & Gontard, 2007; Borlieu, Guillard, Vallès-Pamiès, Guilbert, & Gontard, 2009). For the past 10 years, research on edible films and coatings in foods was driven by food engineers due to the high demand of consumers for longer shelf-life and better quality of fresh foods as well as of environmentally friendly packaging. In addition, edible films and coatings can be used as a vehicle for incorporating natural or chemical antimicrobial agents, antioxidants, enzymes or functional ingredients such as probiotics, minerals and vitamins (Skurtys et al., 2010). Excellent reviews on film-forming food biomaterials and their properties can be found in the recent published literature (Borlieu et al., 2007, 2009; Nussinovitch, 2003; Skurtys et al., 2010). Although the potential of edible films to improve food quality and extend shelf life has been proved, most of the works in this area are focused on the formulation point of view and few studies deals with the effect of the film microstructure on their physical properties.

The barrier (water vapor, O_2, CO_2, *etc.*), mechanical and optical properties of a film are the upmost importance when defining its suitability for a specific target application. Generally, films composed of one substance have either good barrier or good mechanical properties but not both (Borlieu et al., 2009; Callegarin, Quezada

* Corresponding author. Tel.: +56 2 3544264; fax: +56 2 3545803.
E-mail address: rnzuniga@uc.cl (R.N. Zúñiga).

0144-8617/$ – see front matter © 2012 Elsevier Ltd. All rights reserved.
http://dx.doi.org/10.1016/j.carbpol.2012.06.066

Gallo, Debeaufort, & Voilley, 1997). Polysaccharides and proteins create a network responsible for good mechanical properties, but their inherent hydrophilic nature makes them a poor barrier for water vapor transfer. On the contrary, lipids have excellent water vapor barriers because of their hydrophobic character, but films made from lipids alone are usually brittle, opaque, unstable and waxy tasting (Callegarin et al., 1997). Therefore, considerable attention has been focused on the development of composite edible films, which combine the advantages associated of each class of film-formers: the moisture barrier properties of lipids and the ability to form a resistant matrix of the hydrocolloids (Borlieu et al., 2007, 2009; Callegarin et al., 1997; Morillon, Debeaufort, Blond, Capelle, & Voilley, 2002). One approach to design composite films is dispersing a lipid compound into a hydrocolloid film-forming dispersion making an emulsion, which is then cast and dried to prepare an emulsified-film. Emulsified-films are less efficient than bilayers films due to the non-homogeneous distribution of lipids, but they have received more interest because they need only one drying step instead of the two necessary for create bilayer films (Quezada Gallo, Debeaufort, Callegarin, & Voilley, 2000). Goods reviews on lipid-based films can also be found in the recent literature (Callegarin et al., 1997; Morillon et al., 2002).

Many of the most important properties of emulsions are determined by the size of the droplets they contain (Walstra, 2003). Initial characteristics of emulsions (particle size and size distribution) would lead to different microstructures during drying of emulsion-based films, which in turn affects to a greater extent the physical properties of the film. Hence, the emulsion structure has to be controlled during the preparation and formation (drying) of the film. Heat and solvent evaporation during drying of the hydrocolloid-based emulsion induces changes in the initial emulsion structure, particularly driven by destabilization phenomena like creaming, aggregation and/or coalescence (Phan The, Debeaufort, et al., 2002; Phan The, Péroval, et al., 2002). The rearrangement of the oil droplets in the film matrix during the film drying, which defines its internal and surface structure, has an important role in the optical, mechanical and barrier properties of the emulsion-based films.

Controlling the initial structure and some properties of the film-forming emulsion can contributes to the understanding of film properties. The ability of food manufacturers to formulate emulsion-based products with tailored properties depends on knowledge of the relationship between their physical properties and their composition and microstructure (Chanamai & McClements, 2001). Therefore, the objective of this work was to study the effect of the microstructure of oil-in-water emulsions stabilized by hydroxypropyl methylcellulose (HPMC) alone or by HPMC with sodium dodecyl sulfate (SDS) over physical properties of HPMC emulsion-based edible films. This study is an attempt to relate the microstructure of the films with their barrier, mechanical and optical properties. To compare in a more realistic way the treatments, emulsions with two equal droplet size and size distributions were produced, independent of concentration of the dispersed phase used.

2. Materials and methods

2.1. Materials

Hydroxypropyl methylcellulose (HPMC, METHOCEL E19, Dow Wolff Cellulosics, Bomlitz, Germany) was used as the structural material in all formulations due to their excellent film-forming properties (Borlieu et al., 2007; Skurtys et al., 2010). HPMC is a white, odorless and tasteless powder of a water-soluble cellulose derivative. The presence of hydroxypropyl and methyl groups in HPMC renders the cellulose molecule hydrophobic and thus HPMC acquires surface active properties (Petrovic, Sovilj, Katona, & Milanovic, 2010). According to the manufacturer HPMC has a nominal viscosity of 19 mPa s and a number average molecular weight of 16,000. The methoxyl degree of substitution was 1.9 and the hydroxypropyl molar substitution was 8.5. These factors affect the thermal gelation temperature of the aqueous dispersions and the strength of the films formed (Cash & Caputo, 2010). Propylene glycol (PG, LyondellBasell Industries Holdings, Rotterdam, The Netherlands) was incorporated to the formulations because behaves as plasticizer in edible films, giving to the material flexibility and tear resistance (Borlieu et al., 2007). A commercial brand of sunflower oil (Natura™, Argentina) was used as the hydrophobic dispersed phase. Sodium dodecyl sulfate (SDS, Sigma–Aldrich Corp., St. Louis, MO, USA) was used as surfactant in some formulations. All reagents were used as received without further purification.

2.2. Emulsion formation

Different compositions of the film-forming dispersions were formulated according to Table 1. HPMC powder was dispersed in distilled water at 60 °C for 2 h under moderate stirring avoiding foam formation, then PG was incorporated and, finally, depending on the formulation, SDS was added. The dispersion was stirred for 30 min more and left at 4 °C for at least 12 h to allow complete hydration of the polymer. Previous studies has been shown that inter/intra-molecular interactions occur between HPMC and SDS above certain surfactant concentration, *i.e.* critical aggregation concentration (CAC), leading to modification in some physical properties of the system, such as viscosity and surface tension (Katona, Sovilj, Petrovic, Mucic, 2010; Nilsson, 1995; Petrovic et al., 2010). At the SDS concentrations used in this work, probably no interactions occur between the surfactant and the HPMC. Values for CAC were found about 1.0% (w/w) of SDS, below this concentration no interactions occur, independent of the polymer concentration (Nilsson, 1995; Katona et al., 2010). For film-forming emulsions, sunflower oil was added dropwise to dispersions while mixing using a stirring plate at 300 rpm for 1 min at 30 °C, thus forming a coarse emulsion. The oil-to-surfactant mass ratio was 10-to-1 for the SDS stabilized emulsions. In order to decrease the droplet sizes an ultrasonic processor (Branson Sonifier 450, Branson Ultrasonics, Danbury, CT, USA) with a 19 mm (0.75 in.) stainless steel ultrasound probe was used to sonicate 60 g of the coarse emulsion in a 120 ml beaker. The tip horn was adjusted 1 cm below the surface of the sample. Sonication was carried out in the pulsed mode (frequency of one pulse per second, duration of the pulse 0.3 s) at a nominal power level of 250 W for 180 s. Film-forming dispersions were degassed at room temperature with a vacuum pump. All formulations were done in triplicate at the same level of total solids and were named HPMC, HPMC-0.3, HPMC-1.0, HPMC-0.3-SDS and HPMC-1.0-SDS, according to the levels of oil and SDS used (Table 1).

Table 1
Compositions of the film-forming dispersions (%, w/w) for 100 g of dispersion. All dispersions were formulated at the same level of solids.

Film forming dispersion notation	HPMC	PG	Oil	SDS
HPMC	3.50	2.0	–	–
HPMC-0.3	3.20	2.0	0.3	–
HPMC-0.3-SDS	3.17	2.0	0.3	0.03
HPMC-1.0	2.50	2.0	1.0	–
HPMC-1.0-SDS	2.40	2.0	1.0	0.10

HPMC, hydroxypropyl methyl cellulose; PG, propylene glycol; SDS, sodium dodecyl sulfate.

2.3. Interfacial tension measurements

Interfacial tension was measured by the pendant drop method, previously reported (Skurtys & Aguilera, 2009; Skurtys et al., 2011). A small film forming dispersion drop (about 10–20 μl) attached to the tip of a stainless-steel needle (outer diameter of 1.25 ± 0.005 mm) was hung into 10 ml of oil under a constant temperature (21.0 ± 0.1 °C). The drop was formed by a controlled syringe pump (Model 1000, New Era Pump System Inc., Farmingdale, NY, USA). Images of the drop were taken as function of time with a CCD camera (Pulnix model TM-6740GE, Pulnix Inc., San José, CA, USA) with a pixel resolution of 640 × 480 equipped with a zoom objective and operated *via* software. The shape of the drop at equilibrium, determined by the balance of gravity and interfacial tension (γ), was determined from the fundamental Laplace equation:

$$\frac{d\ \sin\theta}{dx} = \frac{2}{b} - \frac{g\Delta\rho}{\gamma}z - \frac{\sin\theta}{x} \quad (1)$$

The origin of the coordinate system was at the drop apex; x and z (m) are the Cartesian coordinates at any point of the droplet, b is the radius of curvature at the apex (m); θ is the angle between the drop axis and the normal to the drop interface, g is the acceleration gravity constant (m/s^2), $\Delta\rho$ is the difference in the densities of the dispersion and air (kg/m^3). To validate the results it was corroborated experimentally that the interfacial tension of the pure water/air system was 72.0 ± 0.3 mN/m.

2.4. Flow properties of film-forming dispersions

The rheological behavior of the film-forming dispersions was determined using a coaxial cylinder geometry in a controlled shear rate rheometer (model DV-III, Brookfield Engineering Laboratories, Stoughton, MA, USA) at 25 °C applying the flow curve method. Shear rate was increased linearly from 0 to 100 s^{-1} in 30 min (upward ramp) and then decreased in a similar way to 0 s^{-1} over 30 min (downward ramp). Experiments were done in triplicate.

2.5. Quantification of emulsion droplet sizes by image analysis

Droplet sizes were determined from images of the emulsions obtained with a light microscope (Olympus model BX50, Olympus Optical Co. Ltd., Tokyo, Japan) and recorded with a digital CCD camera (CoolSnap-Pro Color, Photometrics Roper Division, Inc., Tucson, AZ, USA). Each image (1392 × 1040 pixels) was saved as a 24 bits TIFF image file of approximately 1.38 MB, without compression.

Image processing for droplet size analysis was carried out automatically using a segmentation algorithm developed under Matlab environment (Matlab 7.6 (R2009a), The MathWorks Inc., MA, USA), mainly based on mathematical morphology (Bellalta, Troncoso, Zúñiga, & Aguilera, 2012). Briefly, the data processing of the digitalized images consisted of different steps, including contrast enhancement, different filter operations followed by an automatic segmentation. This procedure allowed considerable reduction of the data analysis time without losing accuracy.

A substantial number of droplets (N = 1000) were counted to obtain statistical estimates of the droplet size distribution in each sample. Volume frequency distributions of droplets were generated by grouping the bubbles into classes belonging to a common interval. The volume frequency of any class interval was computed using MS-Excel (Microsoft™ Excel 2010) as the number of droplets in that class (class frequency) divided by the total number of droplets and expressed as a percentage. The volume-surface mean droplet size ($D_{3,2}$) was calculated using Eq. (2). This value represents the average size based on the specific surface per unit volume and better characterizes small and spherical particles.

$$D_{3,2} = \frac{\sum n_i d_i^3}{\sum n_i d_i^2} \quad (2)$$

where n_i is the number of droplet with diameter d_i (μm).

2.6. Creaming of emulsions

The destabilization of the emulsions produced by gravitational separation (creaming) was evaluated by means of spectrophotometric measurements. Light transmittance was measured at 850 nm using a spectrophotometer (Shimadzu, model UV-160, Kyoto, Japan). Emulsions were contained in plastic cuvettes with a 1 cm path length. Transmittance measurements were made using a standard double-beam arrangement, with the transmittance of the sample being measured relative to that of a reference cell containing distilled water (Chanamai & McClements, 2001). Emulsions contained in the cuvettes were covered with plastic films (*i.e.* Parafilm™), stored at 25 °C and measured at different time intervals. To avoid the effect of differences in the initial transmittance of samples, the results are presented as the ratio between values measured at different times with the initial transmittance (normalized values).

2.7. Film formation

Edible films were obtained by casting 12 g of the film-forming dispersions on leveled acrylic plates (length 10 cm, width 10 cm). Film-forming dispersions were dried by convection in an oven at 40 °C and 23% relative humidity (RH) for 24 h. The films were removed from the oven and immediately placed in a desiccator (25 °C) over a saturated solution of potassium acetate (22% RH) (Sigma–Aldrich Corp., St. Louis, MO, USA) and held for 48 h before testing. Measurements of film thickness were made at 8 positions on each film sample using a digital micrometer, average values were calculated with an accuracy of 0.002 mm.

2.8. Coalescence of emulsion droplets during drying of films

For the evaluation of droplet coalescence during film formation, 0.5 g of the emulsion-based films were dispersed in 10 g of a 0.1% (w/w) SDS solution and stirred at 100 rpm at room temperature for 30 min until complete dissolution of the film. SDS was used in order to avoid droplet coalescence during the dissolution step. Droplet size distributions were obtained in the same way as explained for the emulsions employed to make the films (see Section 2.5). Coalescence was evaluated as the change in $D_{3,2}$ between fresh formed emulsions and the emulsions obtained by dissolving the emulsion-based films.

2.9. Microscopic structure of emulsion-based films

Emulsion-based films were observed under a light microscope (Olympus BX50, Optical Co., Tokyo, Japan) and images were recorded with a digital CCD camera (CoolSnap-Pro Color, Photometrics Roper Division, Inc., Tucson, AZ, USA).

2.10. Scanning Electron Microscopy (SEM) surface analysis of films

SEM was used to characterize qualitatively the surface microstructure of HPMC-based films. The samples were sputter-coated with gold-palladium and examined with a scanning electron microscope (JEOL JSM 5300, Jeol Ltd., Tokyo, Japan), operated at

an acceleration voltage of 20 kV. Micrographs were taken at different magnifications and selected images are reported. ADDA II was used as interface between microscope and computer and the images were analyzed with the software AnalySIS® version 3.2 (Soft Imaging System GmbH, Münster, Germany).

2.11. Transparency of the films

The light barrier properties of films were measured by exposing the films to light at wavelengths ranging from 200 to 900 nm, using a spectrophotometer (Shimadzu, model UV-160, Kyoto, Japan). The film sample was cut into a rectangular shape (40 mm long and 10 mm width) and placed on the internal side of a plastic cuvette, closest to the beam light of the spectrophotometer cell. Transparency of the films was calculated by Eq. (3):

$$T = \frac{Trans_{600}}{x} \tag{3}$$

where $Trans_{600}$ is the transmittance of light through the film at 600 nm and x is the film thickness (mm).

2.12. Instrumental color of the films

Color measurements were done using a tristimulus colorimeter (HunterLab, model ColorFlex, Hunter Associates Laboratory Inc., Reston, VA, USA), applying the CIELab scale. The instrument was standardized each time with a white and black ceramic plate. The whiteness index (WI) was defined as:

$$WI = 100 - \sqrt{(100 - L^*)^2 + a^{*2} + b^{*2}} \tag{4}$$

where L^* (black 0 to white 100), a^* (red 120 to green −120) and b^* (yellow 120 to blue −120) values correspond to whiteness, redness and yellowness, respectively.

Total color difference (ΔE) between control HPMC film (L_0^*, a_0^*, b_0^*) and emulsion-based films (L^*, a^*, b^*) was defined as:

$$\Delta E = \sqrt{(L_0^* - L^*)^2 + (a_0^* - a^*)^2 + (b_0^* - b^*)^2} \tag{5}$$

Measurements of film color were done in triplicate over the same white ceramic plate used for calibration.

2.13. Mechanical properties of the films

Tensile measurements were carried out for films cut in rectangular sections (100 mm long and 30 mm width). Samples were mounted and clamped with grips in a texture analyzer machine (TA.XT2i Texture Analyzer, Stable Micro Systems, Godalming, UK). Grip separation was set at 50 mm and samples were stretched at a constant speed of 0.1 mm/s at 25 °C until break.

The overall stress acting on the sample during tension was expressed as the so-called true normal stress (σ), which is the force normal to the film cross section F (N) divided by the initial area A_0 (m^2) of the sample (Hamann, Zhang, Daubert, Foegeding, & Diehl, 2006):

$$\sigma = \frac{F}{A_0} \tag{6}$$

The elongation of films (E) was expressed as percent of the initial height as follows:

$$E = \frac{H}{H_0} \times 100\% \tag{7}$$

where H_0 and H (m) are the initial and final height of film after deformation, respectively. Tensile properties at break, tensile strength (σ_B) and percent of elongation (E_B), were calculated from stress–distance curves. Measurements were done in cuatriplicate.

Table 2
Surface tension parameters (mJ/m^2) of test liquids as given by Cantin et al. (2006).

Liquids	γ_L	Apolar acid–base		
		γ_{LV}^{LW}	γ_{SV}^{+}	γ_{SV}^{-}
α-Bromonaphthalene	45.0	45.0	0.00	0.0
Diiodomethane	50.8	50.8	0.00	0.0
Ethylene glycol	48.0	29.0	1.92	47.0
Formamide	58.0	39.0	2.28	39.6
Glycerol	64.0	34.0	3.92	57.4

2.14. Surface free energy (SFE) measurements

SFE of films was determined by the contact angle (CA) technique and surface tensions of the probe liquids (Skurtys et al., 2011). CA is defined as the angle between the baseline of the drop and the tangent line drawn at the point of contact of the droplet with the surface, which passes through the triple-point of atmosphere–liquid–solid. Five different liquids (all from Sigma–Aldrich Corp., St. Louis, MO, USA) with known surface tension and surface energy components (Table 2) were used for SFE measurements: α-bromonaphthalene (97%), diiodomethane (99%), ethylene glycol (99.3%), formamide (99%) and glycerol (>99%). They span the whole range of fluids going from apolar to nearly polar (Cantin, Bouteau, Benhabib, & Perrot, 2006). The HPMC-based films were cut into rectangles (50 mm long and 10 mm width) and pasted onto the surface of a microscope glass slide with tape. Drops of each liquid were manually deposited over the film surface using a precision microliter pipette. It is important to stress the well-known fact that the drop deposition is a really critical step and it can be a great source of errors. All the values presented in this work were measured from gently dispensed drops keeping the micropipette perpendicular to the surface. The drop volume (1–2 μl) was sufficiently small to assume the volume forces (effect of gravity) to be negligible on the drop shape. Thus, CA values corresponded to the advancing CAs at equilibrium measured at the end of the spreading process. For each liquid at least 10 right and left CAs were measured at 21.0 ± 0.1 °C. In order to avoid liquid adsorption by the film, the typical CA equilibrium measurement was performed 30 s after the drop placement on the surface. The theoretical considerations and equations to obtain SFE values are presented in detail by Skurtys et al. (2011).

The optical system used to record the drops comprised a CCD camera (Pulnix TM-6740GE, Pulnix Inc., San Jose, CA, USA) with a pixel resolution of 640 × 480 equipped with a zoom video lens (Edmund Optics, NJ, USA) and operated *via* software. CA values were determined using ImageJ program (Rasband, 2007) with the plug-in Drop Shape Analysis (Drop-analysis, 2011). The accuracy of the analysis is high since the plug-in used a method based on B-spline snakes (active contours) (Stalder, Kuli, Sage, Barbieri, & Hoffmann, 2006).

2.15. Water vapor transmission rate (WVTR) and water vapor permeability (WVP) measurements

The *WVTR* was measured gravimetrically using a modification of the "cup method" (Fig. 1) (Gennadios, Weller, & Gooding, 1994). Circular samples were cut from films and mounted in glass cups (transfer area = 3.14×10^{-4} m^2) containing a saturated solution of potassium acetate (22% RH) (Sigma–Aldrich Corp., St. Louis, MO, USA). Silicon sealant (Molykote 11, Dow Corning, Münich, Germany) was used to seal films into the test cups. The cups were weighted and introduced into a desiccator at 25 °C containing a saturated salt solution of barium chloride (90% RH) (Merck, Darmstadt, Germany) to expose the films to a high RH. The side of the film in contact with the acrylic plate during film formation was placed in

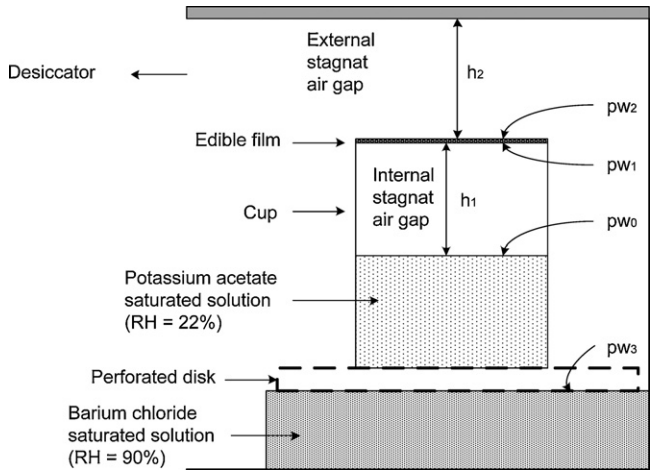

Fig. 1. Scheme of the water vapor permeability cup indicating locations of water vapor partial pressures and stagnant air gap heights.

contact with that part of the test cup having the lower RH. Weight measurements were taken for each cup five times per day for 2 days. Previous tests showed no statistical differences ($p > 0.05$) between weight gain curves obtained at 1, 2, 3 or 4 days.

Weight gain was plotted over time given straight lines ($R^2 > 0.98$). *WVTR* was determined as the ratio between the slope of the weight gain curve (S) and the film area (Eq. (8)):

$$WVTR = \frac{S}{A} \tag{8}$$

where S is the slope of the weight gain against time curve (g/s) and A is exposed film area (m^2).

Stagnant air layers inside and outside the test cup result in significant resistance to water transport (Gennadios et al., 1994; McHugh, Avena-Bustillos, & Krochta, 1993), hence the methodology proposed by Gennadios et al. (1994) was employed for calculating the corrected values of *WVTR* (Eq. (9)) when stagnant air gaps are presented above and below the film (Fig. 1). Detailed information about the equations is given by Gennadios et al. (1994).

$$WVTR_C = WVTR \times \left(\frac{pw_3 - pw_0}{pw_2 - pw_1}\right) \tag{9}$$

where pw_0, pw_1, pw_2 and pw_3 are the partial pressures at the surface of the saturated potassium acetate solution in the cup, at underside of the film, at the film surface outside of the cup and at the surface of the saturated barium chloride solution (Pa), respectively. Corrected water vapor permeability (WVP_C) can be calculated from the following equation:

$$WVP_C = \frac{WVTR_C \times x}{pw_3 - pw_0} \tag{10}$$

2.16. Statistical analysis of data

Analysis of variance (ANOVA) tests were used to analyze the data at a confidence level of 95%, using Statgraphics Plus 5.1 software (Manugistics Inc., Statistical Graphics Corporation, Rockville, USA).

3. Results and discussion

The effect of the emulsion structure over the films properties was studied, to this some emulsion properties were measured and related to the structure of edible films and their effect on films physical properties.

3.1. Microstructure of emulsions

Many of the structural components in food emulsions are in the micron-size range and, therefore, cannot be observed directly

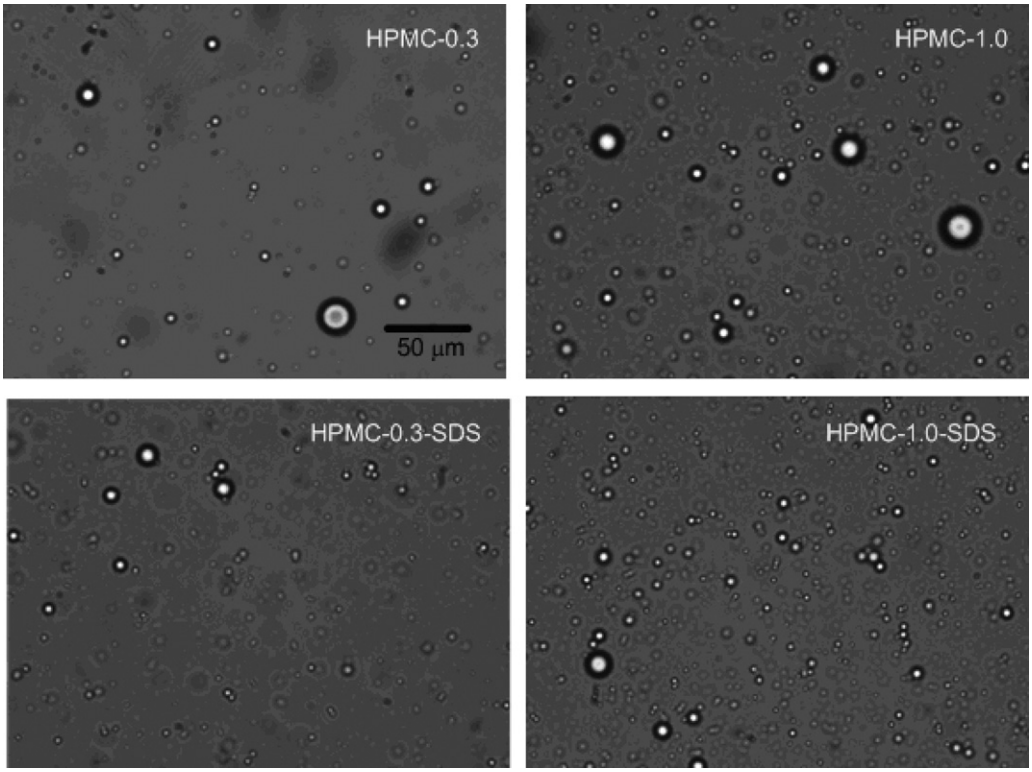

Fig. 2. Gallery of images obtained by optical microscopy of emulsions stabilized by HPMC alone or by HPMC with SDS, showing the similarity between droplet sizes of emulsions with or without SDS. Micrographies are shown without image processing.

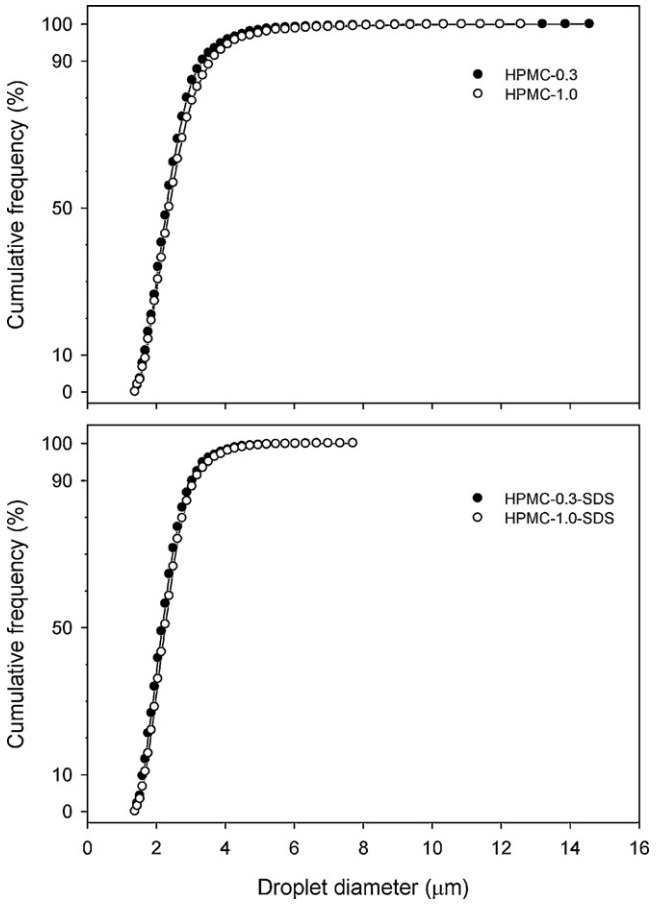

Fig. 3. Effect of oil content and use of surfactant (SDS) on the cumulative droplet size distributions of (A) HPMC and (B) HPMC-SDS stabilized emulsions.

by the eye (*e.g.* emulsion droplets, surfactant micelles, fat crystals and protein aggregates) (McClements, 2005; Walstra, 2003), so microstructural analysis is needed in order to evaluate the microstructure of emulsions and related it with their physicochemical properties.

Monomodal polydisperse emulsions were produced using ultrasound as homogenizing medium. Microscopy images showed a high similarity in droplet sizes of emulsions with (HPMC-0.3-SDS and HPMC-1.0-SDS) and without SDS (HPMC-0.3 and HPMC-1.0), showing only differences in the number of droplets present in the micrographs at 0.3 and 1.0 wt% of oil (Fig. 2). Emulsions formulated with SDS presented smaller droplet sizes and lower dispersions of sizes, independent of the oil concentration used. Image analysis did not show differences between droplet size distributions of emulsions prepared at different oil content. However, by using SDS the droplet size distributions were shifted to lower values (Fig. 3), because the addition of SDS decreased the interfacial tension between oil and HPMC with a value of ~5.8 mN/m, whereas a value of ~13.0 mN/m was measured for HPMC dispersions without surfactant (Table 3). The formation of interfacial tension gradients and the reduction in interfacial tension of the system are important factors during homogenization, because they facilitate the further disruption of emulsion droplets (*i.e.* less energy is required to break up a droplet) and, consequently, lead to emulsions with lower size distributions and higher interfacial area between the oil and water phases (McClements, 2005; Walstra, 2003). Also, SDS prevented the coalescence of newly formed droplets by rapid adsorption and stabilization of the newly formed interface.

The volume-surface mean droplet diameters ($D_{3,2}$) did not present statistical differences ($p > 0.05$) between the oil concentrations used (Fig. 4). The $D_{3,2}$ values were 3.79 and 3.77 μm for HPMC-0.3 and HPMC-1.0 emulsions, respectively, and 2.72 and 2.71 μm for HPMC-0.3-SDS and HPMC-1.0-SDS emulsions.

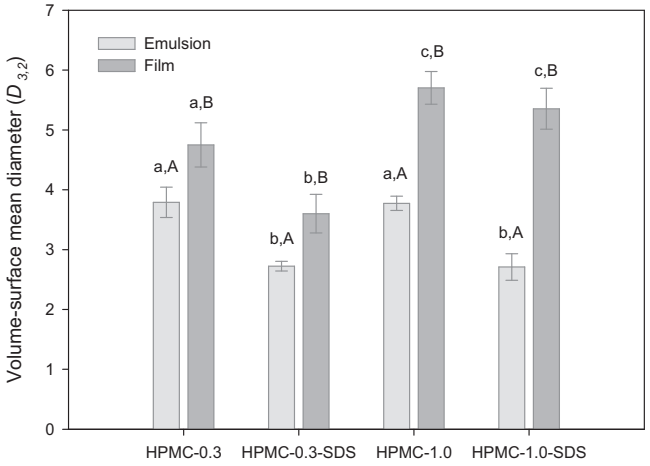

Fig. 4. Effect of oil content and use of surfactant (SDS) on volume-surface mean droplet diameter ($D_{3,2}$) of film forming emulsions and edible films. Different lower case letters indicate significant differences ($p < 0.05$) between formulations and different upper case letters indicate significant differences ($p < 0.05$) between emulsions and films.

3.2. Rheological behavior of film-forming dispersions

All the film-forming dispersions showed a Newtonian behavior and no thixotropic effects were observed from the comparison of the up and down curves. Viscosity of HPMC dispersion was 8.23×10^{-2} Pa s, being higher than the film-forming emulsions (Table 3). Emulsions containing 0.3 and 1.0% of oil had viscosity values of 6.61×10^{-2} and 5.28×10^{-2} Pa s for emulsions formulated without SDS and values of 6.23×10^{-2} and 5.60×10^{-2} Pa s when SDS was incorporated. The incorporation of oil and/or SDS did not promote notable changes in the viscosity of the film forming dispersions in the range of the shear rate analyzed, confirming the assumption that no interactions between polymer and surfactant occurred in these systems. The decrease in viscosity values with an increase in oil content was due to replacing part of the polymer for oil and/or surfactant, which seems to indicate that more free solvent is present in the system when the lipid and/or the surfactant was incorporated, replacing the HPMC (Fabra, Jiménez, Atarés, Talens, & Chiralt, 2009). No effect of droplet size over viscosity values was found, probably because the low oil fraction used in the HPMC-based emulsions. In emulsions with low oil contents, the particles are far apart and the inter-particle interactions are relatively weaker. This structural conformation explains the low viscosity of these systems and their Newtonian behavior.

Table 3
Physical properties of HPMC-based film-forming dispersions.

Film forming dispersion	Interfacial tension ((mN/m)	Viscosity $\mu \times 10^2$ (Pa s)	Film thickness (μm)
HPMC	–	8.23^a	30.5^a
HPMC-0.3	13.0^a	6.61^b	32.5^a
HPMC-0.3-SDS	5.9^b	6.23^c	31.8^a
HPMC-1.0	12.9^a	5.26^e	31.5^a
HPMC-1.0-SDS	5.7^b	5.60^d	30.0^a

Columns with different letters indicate significant differences ($p < 0.05$).

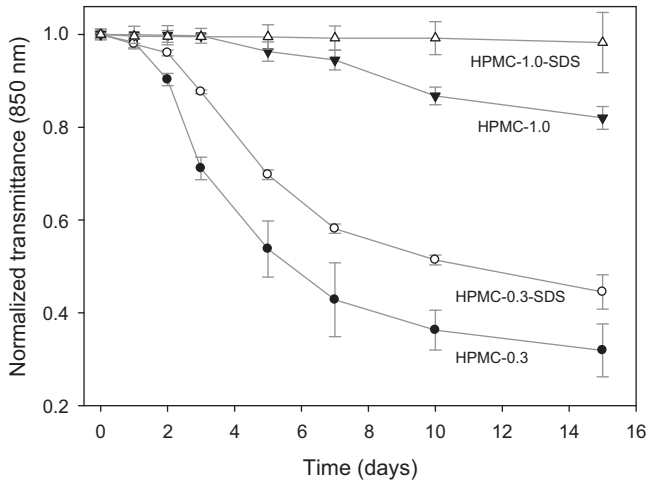

Fig. 5. Effect of oil content and use of surfactant (SDS) on the stability (creaming) of HPMC-based emulsions. Lines are only guide to the eye.

3.3. Destabilization (creaming) of emulsions

Scattering of light, which can be due to reflection, refraction, or diffraction, occurs at sites where the refractive index changes, for instance at the droplet interphase (Walstra, 2003). Therefore, the absorbance of the emulsions at certain height of the container, as a function of time, can be related to the concentration of droplets and thus, to the creaming process. The most important factors for stability of emulsions are the continuous phase rheology, the particle concentration, the particle size distribution and the colloidal interactions between the particles (Chanamai & McClements, 2000).

The degree of scattering by an emulsion depends on the concentration, size and refractive index of the particles present (Chanamai & McClements, 2001). As the droplets moved upwards due to gravity there was a decrease in the absorbance at the bottom of the emulsions, because the local droplet concentration decreased. The curves shown in Fig. 5 indicate that the rate of creaming decreased appreciably when the oil concentration was increased from 0.3 to 1.0% (w/w). The decrease in creaming velocity with increasing droplet concentration could be due to particle–particle interactions (*i.e.* electrostatic repulsion), as stated by Chanamai and McClements (2000). As expected, the creaming was faster in the emulsions containing the larger droplets. HPMC-1.0 and HPMC-1.0-SDS emulsions presented higher stability, with almost no change in absorbance during 3 and 5 days of storage, respectively (Fig. 5). HPMC-0.3 and HPMC-0.3-SDS showed an exponential decay of absorbance with time.

3.4. Formation of edible films

Both HPMC and HPMC emulsion-based films were flexible and easy to handle, while the former was transparent the inclusion of oil produced a loss of transparency (opacity) in a degree dependent on the formulation. No statistical differences ($p > 0.05$) were found between the thickness of edible films (Table 1), so the effect of thickness over color and mechanical properties can be eliminated.

3.5. Microscopic structure of emulsion-based films observed by light microscopy

As stated above, many of the structural components in food emulsions are in the micron-size range, also this is true for emulsion-based edible films. So, the study of the microstructure of this kind of films is crucial to understand and design their physical properties. The effects of oil concentration and the use of SDS on the microstructure of emulsion-based edible films are shown in the micrographs presented in Fig. 6. Emulsion-based films appeared as a continuous matrix of HPMC with a dispersed lipid phase composed of oil droplets and droplet aggregates of different sizes. Different microstructures were obtained for emulsion-based edible films, almost intact oil droplets can be seen for HPMC-0.3, HPMC-0.3-SDS and HPMC-1.0-SDS films, which appear as dark gray circles with a white center. However for HPMC-1.0 films only "oil plates" with an irregular form can be seen, which also appear in the other films, these "oil plates" are coalesced oil droplets produced during film formation. During drying of emulsions water evaporates and instability phenomena occurred (*i.e.* creaming, aggregation and coalescence) being dependent on the concentration of the oil phase and the use of surfactant. Probably, droplets in SDS-stabilized emulsions were prevented from aggregate and coalesce by electrostatic stabilization (Callegarin et al., 1997). Fig. 4 confirms the phenomena of coalescence during film formation, the increase in $D_{3,2}$ values between oil droplets of film forming emulsions and dissolved HPMC emulsion-based films was due to aggregation of two or more oil droplets during drying. The aggregation phenomena during drying of films had been reported for different types of polymers and lipids employed in emulsion-based films (Peroval, Debeaufort, Despré, & Voilley, 2002; Phan The, Debeaufort, et al., 2002; Phan The, Péroval, et al., 2002).

For emulsion-based films without SDS the micrographs in Fig. 6 show larger "oil plates" than for SDS stabilized emulsions. At higher oil concentrations and in the absence of SDS the degree of coalescence was the highest as observed in Figs. 4 and 6. The evaporation of water lead to an increase in the viscosity of the continuous phase and a decrease in the initial thickness of the emulsion layer, then the solidification and shrinking of the continuous phase produces a pressure over the droplets, which initially are enlarged due to the deformation forces and then aggregated leading to the coalescence.

3.6. Surface microscopic structure of HPMC-based films observed by SEM

Creaming phenomena during setting of emulsion-based film produce the migration of oil droplets to the evaporation front, leading to the increase in the roughness of the film surface. In the absence of oil, HPMC films showed a smooth and homogeneous surface. Emulsion-based films without SDS (HPMC-0.3 and HPMC-1.0) presented a rough surface plenty of humps with crater-like holes, whereas HPMC-0.3-SDS and HPMC-1.0-SDS films showed a smoother surface with less-defined protuberances and holes. This difference could affect some surface related properties of the films, like their gloss and water absorption. Similar surface microstructure can be seen in the work of Bosquez-Molina, Guerrero-Legarreta, and Vernon-Carter (2003). As mentioned above, solvent evaporation during the drying of the film-forming emulsion induces changes in the emulsion structure because of destabilization phenomena. The intensity of destabilization depends on the concentration of the lipid, the particle size in the initial emulsion, the use of emulsifiers, the viscosity of the continuous phase, the properties of the interfacial surface of the droplets and drying temperature of films (Phan The, Debeaufort, et al., 2002; Villalobos, Chanona, Hernández, Gutiérrez, & Chiralt, 2005; Fabra, Talens, & Chiralt, 2009). Formation of lipid droplets and their development during film drying suppose the interruption of the hydrocolloid matrix, increasing the internal heterogeneity and the surface roughness of the film (Fabra, Talens, et al., 2009; Villalobos et al., 2005). Deformation of the film surface could be due to the retraction of the HPMC gel network in the emulsion during film-making. Generally, the volume of spreading films

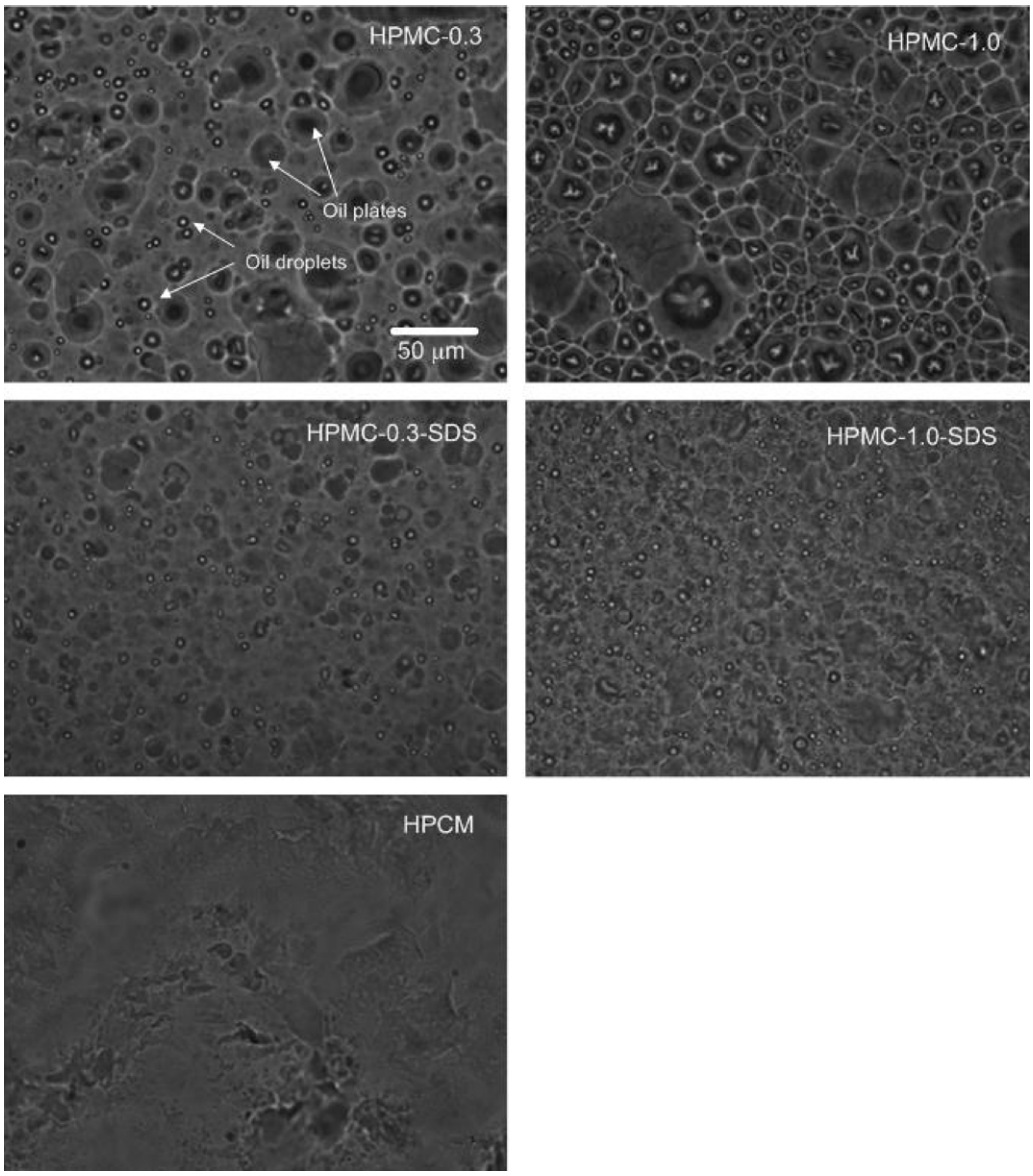

Fig. 6. Gallery of images obtained by optical microscopy of emulsion-based edible films. Image of control film of HPMC is also shown in the figure.

from solution is considerably reduced because of solvent evaporation during drying. This reduction is more remarkable since the film-forming solution sets into a gel, which then retracts on aging. In the case of a cast technique applied for film manufacture, lipid particles should submit to an upright force because the network retraction occurs mainly on the vertical dimension of the film-forming layer (Phan The, Debeaufort, Voilley, & Luu, 2009). From Fig. 7 is clear that an interaction between HPMC, the surfactant and oil produced a smoother surfaced compared with films without SDS.

It has been demonstrated that the cross-sectional structure of emulsion-based film depends on the use of surfactant. Phan The, Debeaufort, et al. (2002) and Phan The, Péroval, et al. (2002) showed by ESEM that in absence of emulsifier the lipid dispersed phase creamed forming an apparent bilayer structure, whereas using sucroester emulsifier at 2.5% films presented an homogeneous structure with a small size of lipid droplets. In agreement with these results, Sánchez-González, Vargas, González-Martínez, Chiralt, and Cháfer (2009) showed that using HPMC, Tween 85 and oil the internal structure of the films presented a homogeneous distribution of droplets.

3.7. Surface free energy (SFE) of edible HPMC-based films

Pseudo-equilibrium CA measurement is an established technique to evaluate surface free energy (SFE) of flat solid surfaces (Skurtys et al., 2011), which has been used as an important indication of the film hydrophobicity. Generally, hydrocolloids films with higher water CA values exhibit a higher surface hydrophobicity (*i.e.* water repellent), thus having better potential to overcome the limitation of this property. The SFE of HPMC film (42.2 mJ/m^2) was almost equal to the value of 43 mJ/m^2 obtained by Fahs, Brogly, Bistac, and Schmitt (2010). Although HPMC film presented the lowest value for the apolar component and the highest value for the polar component, similar values of SFE were found between all films tested, being all low energy surfaces (Table 4). The oil content or the incorporation of SDS had no effect over the SFE values. Emulsion-based films had mainly an apolar character with a small polarity, which represents hydrophobic and hydrophilic character of the film surface, respectively. Apolar surfaces are surfaces where hydrophobicity is observed; the interactions among the water molecules themselves exceed the water-surface interactions (Skurtys et al., 2011). From SFE values presented in Table 4 we

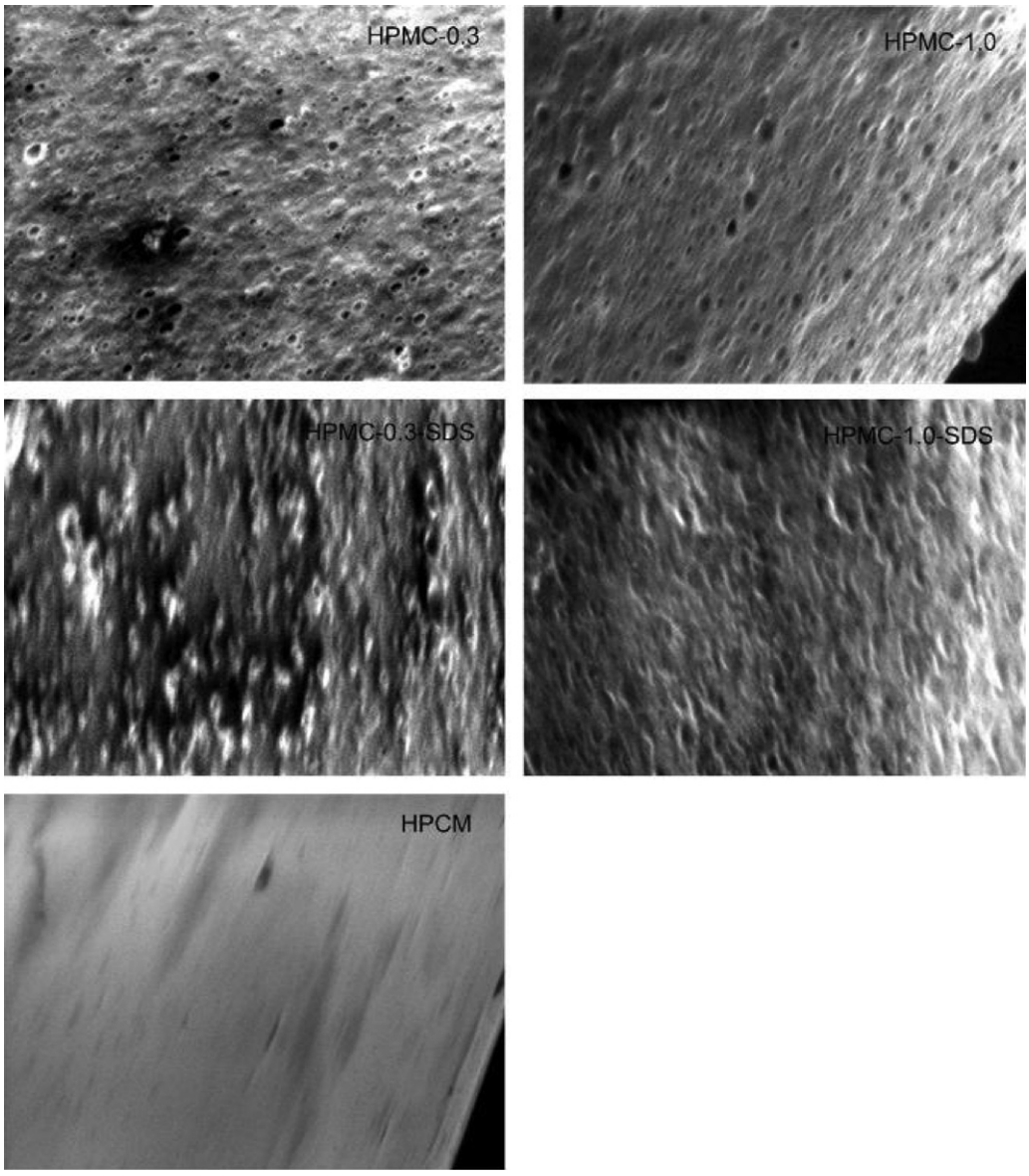

Fig. 7. Gallery of images obtained by SEM of emulsion-based edible films. Image of control film of HPMC is also shown in the figure.

Table 4
Surface free energy (SFE) of HPMC edible films with its apolar and polar components (mJ/m^2).

Edible film	Apolar component γ_{SV}^{d}	Polar component γ_{SV}^{p}	SFE γ_{SV}
HPMC	38.7	3.5	42.2
HPMC-0.3	40.0	1.7	41.7
HPMC-0.3-SDS	41.5	2.2	43.7
HPMC-1.0	40.0	2.8	42.8
HPMC-1.0-SDS	40.5	2.2	40.7

would expect a finite CA and therefore low wetting of film surface with water.

For emulsion-based films, reorientation of the polymer chains (with their polar groups rejected toward the surface of the air), surface roughness and oil migration to the film surface has been suggested as cause of differences in CA and SFE observed for different formulations (Fahs et al., 2010; Karbowiak, Debeaufort, Champion, & Voilley, 2006). Probably, in our case the surface of emulsion-based films is composed by a continuous layer of HPMC around the oil droplets, hence the increase in surface roughness for emulsified HPMC films produce compensation in the apolar and polar components giving the similar SFE values found in this work for all films.

3.8. Color and transparency of edible HPMC-based films

When light of a specific wavelength strikes an object, it may be reflected, transmitted, or absorbed. In addition, scattering of light, which can be due to reflection, refraction, or diffraction, occurs at sites where the refractive index changes (McClements, 2005; Walstra, 2003), for instance at the droplet interphase of composite films. The appearance of films depends on its ability to scatters and absorbs light waves in the visible region of the electromagnetic spectrum. Scattering and absorption determines 'transparency' or 'opacity' and the 'chromaticness' (*e.g.* blueness, greenness, redness or yellowness) of a composite film. A film is said to be transparent when the light impinging on it passes through with a minimum reflection and absorption. In composite films containing immiscible components, the particle size of dispersed phase, the heterogeneity of its distribution and the differences between the refractive indexes of the phases affect the extent of light scattering, and hence the film transparency (Fabra, Talens, et al., 2009).

The internal and surface film microstructure plays an important role in optical properties of the film. According to Villalobos et al. (2005) the transparency of emulsion-base films is related to their internal structure, which is greatly affected by the initial structure of the emulsions (*e.g.* oil volume fraction and droplet size distribution) and their development during drying. Hence, the transmittance of light through emulsion-based films can be related to the concentration of droplets and also to the microstructure of the films. The degree of transparency (T) of emulsion-based films depended on particle size distribution and oil content. The decrease in T for HPMC-0.3 and HPMC-1.0 emulsions-based films was 38% and 70%, in comparison with HPMC film (control film), respectively (Fig. 8A). In turn, diminution in T for HPMC-0.3-SDS and HPMC-1.0-SDS emulsion-based films was 13% and 11%. Film T decreased with increasing droplet concentration because the higher number of discontinuities in the refractive index through the film, in other words more light was scattered by the droplets and therefore less light was transmitted through the emulsions (Chanamai & McClements, 2001; Fabra, Talens, et al., 2009; Villalobos et al., 2005). The incorporation of oil produced an increase in the white index (WI) of the emulsion-based films with respect to the control HPMC film, consequently leading to a change in the color (ΔE) of these films (Fig. 8B and C). The effect of oil content and incorporation of SDS showed the same trend for both WI and ΔE, the increasing order of change, for WI and ΔE, among the formulations evaluated was: HPMC-0.3-SDS > HPMC-1.0-SDS > HPMC-0.3 > HPMC-1.0. The decreasing in T and the increasing in WI and ΔE are clearly related to the light-scattering effect of oil. The "oil plates" formed during drying produced a higher scattering of light, decreasing its transmittance and hence diminishing the transparency of the emulsion-based films and also changing their color. Although HPMC-0.3-SDS and HPMC-1.0-SDS films have a different oil concentration in their structure, the small droplet sizes and their spatial distribution produced very similar optical properties. Clearly, the effect of droplet sizes was more important than the concentration of oil over the optical properties of emulsion-based films.

3.9. Mechanical properties of the films

Mechanical properties on tension were affected by the oil content incorporated into the edible HPMC films. The addition of oil at 0.3% did not have a significant effect ($p < 0.05$) on changing the σ_B values, when comparing with pure HPMC films (Table 5). However, the incorporation of oil at 1.0% diminished significantly the σ_B values of the emulsion-based films. The replace of HPMC by oil at 1.0% produced a lower "amount" of network structure in the films, leading to a weakening of their structure. In addition, the oil may act as structural defects decreasing the strength of films. Crack propagation in a complex structure is highly dependent on interfacial properties and defects, and the heterogeneity of the structure. No significant differences were found between σ_B values for films with and without SDS, thus the incorporation of SDS did not change the mechanical properties of the films, probably SDS did not produced a strong link between the continuous and dispersed phases of the emulsion-based films. The addition of oil decreased significantly ($p > 0.05$) the percent of elongation at break (E_B) in comparison to HPMC film (Table 5). However, differences in composition had no effect over E_B for emulsion-based films.

Most authors had found that the inclusion of lipid particles impaired the mechanical properties of emulsion-based films when comparing with the corresponding hydrocolloid film (Peroval et al., 2002; Phan The, Debeaufort, et al., 2002). Sánchez-González et al. (2009) found a decrease in tensile strength with an increase in the concentration of oil added to HPMC films, but the E_B was kept constant, while the force-at-breaking and E_B of MC emulsion-based films did not show significant differences at different lipid phase content (Quezada Gallo et al., 2000). Oil addition induces development of a heterogeneous film structure featuring discontinuities in the polymer network. These discontinuities reduced the film resistance to fracture with the concomitant decrease in film strength.

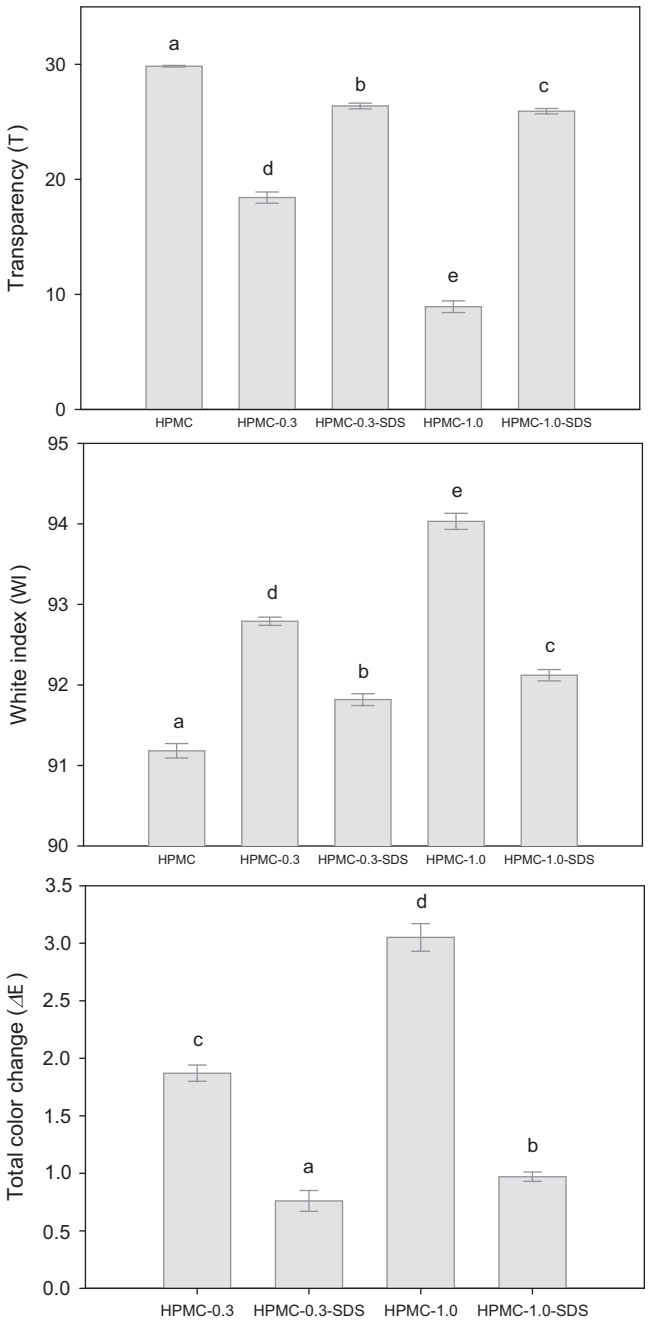

Fig. 8. Effect of oil content and addition of surfactant (SDS) on optical properties of edible films. Different letters indicate significant differences ($p < 0.05$) between formulations.

3.10. Water vapor transmission rate (WVTR) and water vapor permeability (WVP) measurements

Water vapor transfer of edible films is an important property related with the ability of the film to control moisture transfer between the food and their environment. *WVTR* and *WVP* values

Table 5
Mechanical and water vapor barrier properties of HPMC edible films.

Edible film	Mechanical properties		Vapor barrier properties	
	Strength at break σ_B (MPa)	Elongation at break E_B (%)	$WVTR_C$ ($\times 10^{-2}$ g/m^2 s)	WVP_C ($\times 10^{14}$ g/m s Pa)
HPMC	38.4 ± 3.9^a	90 ± 16^a	1.49 ± 0.10^a	2.4 ± 0.2^a
HPMC-0.3	38.2 ± 4.5^a	61 ± 5^b	1.28 ± 0.16^b	2.1 ± 0.3^{ab}
HPMC-0.3-SDS	33.3 ± 2.3^{ab}	64 ± 15^b	1.12 ± 0.14^b	1.8 ± 0.2^b
HPMC-1.0	28.2 ± 3.1^{bc}	58 ± 5^b	0.90 ± 0.11^c	1.4 ± 0.2^c
HPMC-1.0-SDS	23.9 ± 4.0^c	50 ± 10^b	0.67 ± 0.11^d	1.1 ± 0.2^c

$WVTR_C$, water vapor transfer rate corrected; WVP_C, water vapor permeability corrected.
Columns with different letters indicate significant differences ($p < 0.05$).

were corrected taking into account the stagnant air layers above and below the film, as stated in the point 2.15 of Section 2. $WVTR_C$ was significantly ($p > 0.05$) higher for HPMC films and decreased with an increase in the oil content, higher concentration of oil decreased $WVTR_C$ due to the hydrophobic nature of oil. No effect of SDS over $WVTR_C$ could be seen at the lower content of oil, however, at 1.0% of oil the addition of surfactant decrease the $WVTR_C$ of the films (Table 5).

Distribution of oil droplets in the film matrix is critical to water vapor transfer. Microstructure of films had a great impact over $WVTR_C$, because for emulsified films the water transfer occurs through the matrix formed by the hydrophilic polymer (Morillon et al., 2002). According to the tortuosity model, a large number of droplets uniformly dispersed in the hydrocolloid matrix increases the distance traveled by water molecules diffused through the film. No significant differences were found for $WVTR_C$ ($p < 0.05$) for HPMC-0.3 and HPMC-0.3-SDS films. Although HPMC-0.3-SDS emulsions presented a lower particle size distribution (Fig. 3) and its degree of coalescence was lower than HPMC-0.3 emulsions (Fig. 4), leading at different film microstructures during drying (Fig. 6), the low oil content of this films could not produce a significant difference in $WVTR_C$ because water diffuses through the hydrocolloid matrix and, probably, the differences in the tortuosity of the path is not enough to induce a depression in $WVTR_C$ values. In addition, the hydrophilic character of SDS can increase the $WVTR_C$ values for HPMC-0.3-SDS films.

Although Fig. 6 shows a higher amount of "oil plates" for HPMC-1.0 than for HPMC-1.0-SDS films, the $WVTR_C$ of the former was lower; this could be explained because the higher stability of SDS stabilized film-forming emulsion during drying. Lower creaming of HPMC-1.0-SDS (Fig. 5) could produce a homogeneous three dimensional film structure, leading to higher tortuosity of the path for vapor transmission, which could diminish the $WVTR_C$. Creaming and coalescence produced during drying of emulsion (film formation) changes the initial droplet size distribution and could produce an "apparent bilayer structure", which can decrease the *WVTR* and the *WVP* of films, making the films more effective against mass transfer (Morillon et al., 2002; Phan The, Debeaufort, et al., 2002). However, if this "apparent bilayer structure" is not formed, the efficacy of the film is very similar to the hydrocolloid matrix. Our results suggest (Table 5 and Fig. 6) that although HPMC-1.0 films presented a higher coalescence and much evident formation of "oil plates" their affectivity against water vapor transfer was almost equal to HPMC-1.0-SDS films, because in emulsified film water molecules hydrates and diffuses through the continuous hydrophilic matrix and the dispersed lipid phase only modifies the "apparent tortuosity" of the film (Morillon et al., 2002). This can explain why $WVTR_C$ was statistically ($p < 0.05$) lower for HPMC-1.0-SDS than for HPMC-1.0, higher creaming and coalescence stability of HPMC-1.0-SDS produced a more homogeneous three-dimensional structure of the film, leading to a higher "apparent tortuosity".

Surface hydrophobicity has been used as an important indication of hydrocolloid film sensitivity to moisture, and low surface hydrophobicity may correspond to high *WVTR* values, as expected for polar supports. We did not found a relationship between SFE and *WVTR*. Same results were found by Wong, Gastineau, Gregorski, Tillin, and Pavlath (1992) and Peroval et al. (2002), in fact the emulsion-based film most efficient against vapor transfer presented the lowest surface hydrophobicity. Phan The, Péroval, et al. (2002) suggested that the microstructure of films is more important than the surface properties when trying to understand the factors affecting the vapor transfer through emulsion-based films. In the work of Martin-Polo, Maugin, and Voilley (1992) the surface of emulsified films was irregular with spherical masses not well incorporated into the bulk of the film. Their results showed that the ability of the hydrophobic substances to retard moisture transfer depends on the homogeneity of its final repartition in the matrix and/or on the surface.

The *WVP* of a film is a steady state property which describes the rate of water which passes through the film submitted to a given RH difference (Borlieu et al., 2009). Permeability depends on diffusion (kinetic factor) and on sorption (thermodynamic factor) of the penetrant, being water the most common diffusing molecule (Callegarin et al., 1997). The trend for WVP_C values was very similar to that of $WVTR_C$. So, the above discussion for the *WVTR* can be applied to *WVP*. Water vapor transfer through hydrophilic films are dependent on the partial pressure gradients, hence permeability is not an inherent property of hydrophilic films (McHugh et al., 1993). Therefore, permeability values present in this work only can be compared under the same experimental conditions.

4. Conclusions

In this study, HPMC-based edible films were prepared and characterized to obtain information about the relationship between microstructure and the physical properties of these films. Initial microstructure (droplet size distribution) and stability (creaming) of film forming emulsions lead to different surface and internal microstructure of the films. Optical properties of emulsion-based HPMC films were strongly affected by the way that oil droplets were structured into the film. The use of SDS stabilized the emulsion droplets during drying, as confirmed by the microscopic analyses. The mechanical properties of HPMC were affected by formulation, the tensile strength decreased with both the oil content and incorporation of SDS, whereas the elongation at break decreased by one third when oil was incorporated. The increasing order of vapor barrier among the formulations evaluated was: HPMC-1.0-SDS > HPMC-1.0 > HPMC-0.3-SDS > HPMC-0.3 > HPMC. Unstable emulsion (without SDS) with higher coalescence, did not give a better film barrier than films from a stable emulsion, probably because an "apparent" bilayer was not formed at the oil contents used and the hydrophilic HPMC matrix still dominates the vapor transfer. Although SDS has a strong

effect on the microstructural and optical properties of the films, it did not impair the mechanical properties and vapor properties of the films. Finally, no correlation was found between the superficial microstructure and surface free energy or water vapor transfer rate of HPMC-based films.

Acknowledgements

RN Zúñiga thanks to the financial support of the DIPEI of the Pontificia Universidad Católica de Chile and the INNOVA CORFO project 08-CT11-PUT20 Preservation of Quality and Shelf-life Extension of Fresh Blueberries using Edible Films. Special thanks to Dr. Loreto Muñoz for images from SEM. Discussions with Dr. Cristian Ramírez and Dr. Elizabeth Troncoso about methodology and experimental results are always greatly appreciated.

References

Bellalta, P., Troncoso, E., Zúñiga, R. N., & Aguilera, J. M. (2012). Rheological and microstructural characterization of WPI-stabilized O/W emulsions exhibiting time-dependent flow behavior. *LWT-Food Science and Technology*, *46*, 375–381.

Borlieu, C., Guillard, V., Vallès-Pamiès, B., & Gontard, N. (2007). Edible moisture barriers for food product stabilization. In J. M. Aguilera, & P. J. Lillford (Eds.), *Food materials science. Principles and practice* (pp. 547–575). New York: Springer.

Borlieu, C., Guillard, V., Vallès-Pamiès, B., Guilbert, S., & Gontard, N. (2009). Edible moisture barriers: How to assess of their potential and limits in food products shelf-life extension? *Critical Reviews in Food Science and Nutrition*, *49*, 474–499.

Bosquez-Molina, E., Guerrero-Legarreta, I., & Vernon-Carter, E. J. (2003). Moisture barrier properties and morphology of mesquite gum-candelilla wax based edible emulsion coatings. *Food Research International*, *36*, 885–893.

Callegarin, F., Quezada Gallo, J. A., Debeaufort, F., & Voilley, A. (1997). Lipids and biopackaging. *Journal of the American Oil Chemists' Society*, *74*, 1183–1192.

Cantin, S., Bouteau, M., Benhabib, F., & Perrot, F. (2006). Surface free energy evaluation of well-ordered Langmuir–Blodgett surfaces: Comparison of different approaches. *Colloids and Surfaces A: Physicochemical and Engineering Aspects*, *276*, 107–115.

Cash, M. J., & Caputo, S. J. (2010). Cellulose derivatives. In A. Imeson (Ed.), *Food Stabilisers, Thickeners and Gelling Agents* (pp. 95–115). Oxford: John Wiley and Sons.

Chanamai, R., & McClements, D. J. (2000). Dependence of creaming and rheology of monodisperse oil-in-water emuldions on droplet size and concentration. *Colloids and Surfaces. A: Physicochemical and Engineering Aspects*, *172*, 79–86.

Chanamai, R., & McClements, D. J. (2001). Prediction of emulsion color from droplet characteristics: Dilute monodisperse oil-in-water emulsions. *Food Hydrocolloids*, *15*, 83–91.

Drop-analysis (2011). http://bigwww.epfl.ch/demo/dropanalysis. Accessed October, 2011.

Fabra, M. J., Jiménez, A., Atarés, L., Talens, P., & Chiralt, A. (2009). Effect of fatty acids and beeswax addition on properties of sodium caseinate dispersions and films. *Biomacromolecules*, *10*, 1500–1507.

Fabra, M. J., Talens, P., & Chiralt, A. (2009). Microstructure and optical properties of sodium caseinate films containing oleic acid–beeswax mixtures. *Food Hydrocolloids*, *23*, 676–683.

Fahs, A., Brogly, M., Bistac, S., & Schmitt, M. (2010). Hydroxypropyl methylcellulose (HPMC) formulated films: Relevance to adhesion and friction surface properties. *Carbohydrate Polymers*, *80*, 105–114.

Gennadios, A., Weller, C. L., & Gooding, C. H. (1994). Measurement errors in water vapor permeability of highly permeable, hydrophilic edible films. *Journal of Food Engineering*, *21*, 395–409.

Hamann, D. D., Zhang, J., Daubert, C. R., Foegeding, E. A., & Diehl, K. C. (2006). Analysis of compression, tension and torsion for testing food gel fracture properties. *Journal of Texture Studies*, *37*, 620–639.

Karbowiak, T., Debeaufort, F., Champion, D., & Voilley, A. (2006). Wetting properties at the surface of iota-carrageenan-based edible films. *Journal of Colloid and Interface Science*, *294*, 400–410.

Katona, J. M., Sovilj, V. J., Perovic, L. B., & Mucic, N. Z. (2010). Tensiometric investigation of the interaction and phase separation in a polymer mixture-ionic surfactant ternary system. *Journal of the Serbian Chemical Society*, *75*, 823–831.

Martin-Polo, M., Maugin, C., & Voilley, A. (1992). Hydrophobic films and their efficiency against moisture transfer. 1. Influence of the film preparation technique. *Journal of Agricultural and Food Chemistry*, *40*, 407–412.

McClements, D. J. (2005). *Food emulsions. Principles, practice and techniques* (2nd ed.). Boca Raton: CRC Press.

McHugh, T. H., Avena-Bustillos, R., & Krochta, J. M. (1993). Hydrophilic edible films: Modified procedure for water vapor permeability and explanation of thickness effects. *Journal of Food Science*, *58*, 899–903.

Morillon, V., Debeaufort, F., Blond, G., Capelle, M., & Voilley, A. (2002). Factors affecting the moisture permeability of lipid-based edible films: A review. *Critical Reviews in Food Science and Technology*, *42*, 67–89.

Nilsson, S. (1995). Interactions between water-soluble cellulose derivatives and surfactants. 1. The HPMC/SDS/water system. *Macromolecules*, *28*, 7837–7844.

Nussinovitch, A. (2003). *Water-soluble polymer applications in food*. Oxford: Blackwell Science Ltd.

Peroval, C., Debeaufort, F., Despré, D., & Voilley, A. (2002). Edible arabinoxylan-based films. 1. Effects of lipid type on water vapor permeability, film structure, and other physical characteristics. *Journal of Agricultural and Food Chemistry*, *50*, 3977–3983.

Phan The, D., Debeaufort, F., Péroval, C., Despré, D., Courthaudon, J. L., & Voilley, A. (2002). Arabinoxylan-lipids-based edible films and coatings. 3. Influence of drying temperature on film structure and functional properties. *Journal of Agricultural and Food Chemistry*, *50*, 2423–2428.

Phan The, D., Péroval, C., Debeaufort, F., Despré, D., Courthaudon, J. L., & Voilley, A. (2002). Arabinoxylan-lipids-based edible films and coatings. 2. Influence of sucroester nature on the emulsion structure and film properties. *Journal of Agricultural and Food Chemistry*, *50*, 266–272.

Phan The, D., Debeaufort, F., Voilley, A., & Luu, D. (2009). Influence of hydrocolloid nature on the structure and functional properties of emulsified edible films. *Food Hydrocolloids*, *23*, 691–699.

Petrovic, L. B., Sovilj, V. J., Katona, J. M., & Milanovic, J. L. (2010). Influence of polymer surfactant interactions on o/w emulsion properties and microcapsule formation. *Journal of Colloid and Interface Science*, *342*, 333–339.

Quezada Gallo, J. A., Debeaufort, F., Callegarin, F., & Voilley, A. (2000). Lipid hydrophobicity, physical state and distributions effects on the properties of emulsion-based edible films. *Journal of Membrane Science*, *180*, 37–46.

Rasband, W. (2007). Imagej. http://rsb.info.nih.gov/ij/index.html. Accessed October, 2011.

Sánchez-González, L., Vargas, M., González-Martínez, C., Chiralt, A., & Cháfer, M. (2009). Characterization of edible films base don hydroxypropylmethylcellulose and tea tree essential oil. *Food Hydrocolloids*, *23*, 2102–2109.

Stalder, A., Kuli, G., Sage, D., Barbieri, L., & Hoffmann, P. (2006). A snake-based approach to accurate determination of both contact points and contact angles. *Colloids and Surfaces A: Physicochemical and Engineering Aspects*, *286*, 92–103.

Skurtys, O., & Aguilera, J. M. (2009). Formation of O/W macroemulsions with a circular microfluidic device using saponin and potato starch. *Food Hydrocolloids*, *23*, 1810–1817.

Skurtys, O., Acevedo, C., Pedreschi, F., Enrione, J., Osorio, F., & Aguilera, J. M. (2010). Food hydrocolloid edible films and coatings. In C. Hollingworth (Ed.), *Food hydrocolloids: Characteristics, properties and structures* (pp. 41–80). New York: Nova Publishers.

Skurtys, O., Velásquez, P., Henriquez, O., Matiacevich, S., Enrione, J., & Osorio, F. (2011). Wetting behavior of chitosan solutions on blueberry epicarp with or without epicuticular waxes. *LWT-Food Science and Technology*, *44*, 1449–1457.

Villalobos, R., Chanona, J., Hernández, P., Gutiérrez, G., & Chiralt, A. (2005). Gloss and transparency of hydroxypropyl methylcellulose films containing surfactants as affected by their micrsotructure. *Food Hydrocolloids*, *19*, 53–61.

Walstra, P. (2003). *Physical chemistry of foods*. New York: Marcel Dekker Inc.

Wong, D. W. S., Gastineau, F. A., Gregorski, K. S., Tillin, S. J., & Pavlath, A. E. (1992). Chitosan-lipid films: Microstructure and surface energy. *Journal of Agricultural and Food Science*, *40*, 540–544.